Journal of chemical & engineering data

Article

Cite This: J. Chem. Eng. Data 2019, 64, 3436−3443

pubs.acs.org/jced

Measurements of the Solid−Liquid Phase Equilibria in Quinary System NaBr−KBr−$MgBr_2$−$SrBr_2$−H_2O at 323 K

Guo-Liang Nie,[†,‡] Shi-Hua Sang,*[,†,‡] and Rui-Zhi Cui[†,‡]

[†]College of Materials, Chemistry & Chemical Engineering, Chengdu University of Technology, Chengdu 610059, P. R. China

[‡]Mineral Resources Chemistry Key Laboratory of Sichuan Higher Education Institutions, Chengdu 610059, P. R. China

ABSTRACT: In view of the characteristic of the deep underground brine that is rich in sodium, potassium, magnesium, calcium, strontium, chlorine, and bromide in the Sichuan basin, solid−liquid equilibria in quinary system NaBr−KBr−$MgBr_2$−$SrBr_2$−H_2O were accurately determined at 323 K by the method of isothermal dissolution equilibrium. According to the experimental data, the three-dimensional equilibrium phase diagram was obtained. It consists of ten univariant curves, three invariant points, and six crystallization regions. The solids in crystallization regions correspond to NaBr·$2H_2O$, NaBr, $SrBr_2$·$6H_2O$, $MgBr_2$·$6H_2O$, KBr, and KBr·$MgBr_2$·$6H_2O$, of which $MgBr_2$·$6H_2O$ has the minimum crystallization region and KBr has the largest crystallization region, which is bigger than half of the phase diagram. In addition, two-dimensional projections of the saturation surfaces of KBr, $SrBr_2$·$6H_2O$, and $MgBr_2$·$6H_2O$ were also analyzed.

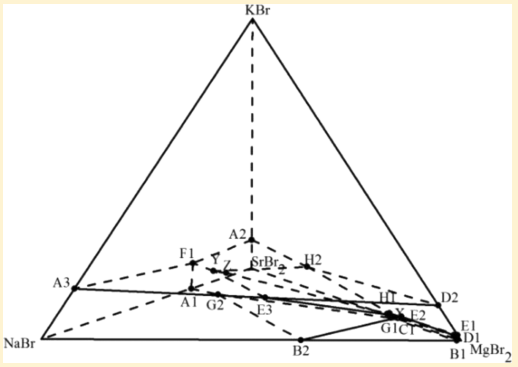

1. INTRODUCTION

The Sichuan basin, a large marine sedimentary basin in the inland of China, is rich in underground brine resources. According to incomplete statistics, there are abundant bittern reservoirs from Sinian to Cretaceous with a wide distribution region and high grades, which is an important enrichment area of liquid mineral resources in the inland of China. The deep underground brine in the western Sichuan basin contains not only the common sodium and chloride elements but also high-grade potassium, bromine, iodine, boron, lithium, strontium, and cesium elements and other useful components, of which potassium, bromide, strontium, and some other elements exceed the grades of industrial exploitation and utilization.[1,2]

Strontium, as a trace element, is essential for the human body. It has been widely used in electronics, metallurgy, military industry, energy, and many other fields due to its distinct chemical properties, with increasingly extensive applications in high-end manufacturing.[3] Potassium is increasingly needed in the industry and agriculture and is also considered as a food of agriculture. Potassium salts are important production materials of potassium-containing chemicals all over the world,[4] about 80% of which is reserved in salt-lake brine and underground brine according to the latest geological surveys. Bromine, an important industrial raw material, is widely used in the preparation of pharmaceuticals, dyes, flame retardants, and pesticides and other fields; furthermore, its application field is continuously extending with the development of the modern pharmaceutical and chemical industry.[5] However, due to its high chemical activity, bromine has no independent minerals in nature but widely exists in liquid mineral resources, such as seawater, underground brine, and salt-lake brine in the form of ions. Therefore, it is of great practical significance to strengthen the comprehensive development and utilization of brine resources for reducing the shortage of solid mineral resources.[6]

The basic theories and data of phase equilibria and phase diagrams are important for revealing the formation and evolution of underground brine, salt mineral deposits, and ancient climate changes. They also have an important significance to guide the development and utilization of brine resources. Meanwhile, they play a key role in environmental protection during the development of various inorganic minerals.[7,8]

As early as in the 1950s, some phase equilibrium studies on water−salt systems containing strontium were carried out.[9−12] These systems include some subsystems of the Na−K−Ca−Mg−Sr−Cl−H_2O system. The Soviet Union scholars completed phase equilibrium studies of ternary systems LiCl−$SrCl_2$−H_2O, NaCl−$SrCl_2$−H_2O, and NaCl−$SrCl_2$−H_2O at 298 K.[13,14] Some Chinese scholars studied the phase equilibria in ternary systems NaCl−$SrCl_2$−H_2O, KCl−$SrCl_2$−H_2O, and $CaCl_2$−$SrCl_2$−H_2O at 298 K,[15−17] aiming at the characteristic of high concentration of strontium in the Nanyishan oilfield water of the Qaidam basin, Qinghai Province. Our group conducted phase equilibrium studies of ternary systems NaCl−$SrCl_2$−H_2O and KCl−$SrCl_2$−H_2O at 323 K,[18] considering the abundant sodium, potassium, magnesium, calcium, strontium, chlorine, and bromide in the deep underground brine of the Sichuan basin. For the systems containing strontium bromide, phase equilibrium studies of ternary system $MgBr_2$−$SrBr_2$−

Received: March 13, 2019
Accepted: July 12, 2019
Published: July 25, 2019

DOI: 10.1021/acs.jced.9b00225
J. Chem. Eng. Data 2019, 64, 3436−3443

Table 1. Chemical Sample Specifications

chemical name	CAS Reg. no.	suppliers	initial mass fraction purity	purification method	analysis method
magnesium bromide hexahydrate	13446-53-2	Shanghai Haorui Chemical Co., Ltd	≥0.990	none	titration
strontium bromide hexahydrate	7789-53-9	Shanghai Haorui Chemical Co., Ltd	≥0.990	none	titration
sodium bromide	7647-15-6	Sinopharm Chemical Reagent Co., Ltd	≥0.990	none	titration
potassium bromide	7758-02-3	Sinopharm Chemical Reagent Co., Ltd	≥0.990	none	titration

Table 2. Compositions of Liquids in Quinary System NaBr−KBr−$MgBr_2$−$SrBr_2$−H_2O and Its Quaternary and Ternary Subsystems at 323 K and 0.09575 MPa[a]

		composition of solution 100 × w(B)[a]				Jänecke index of dry salt J(NaBr)+J(KBr)+J($MgBr_2$)+J($SrBr_2$) = 100			
no.	system	w(NaBr)	w(KBr)	w($MgBr_2$)	w($SrBr_2$)	J(NaBr)	J(KBr)	J($MgBr_2$)	equilibrium solids
A1	NSB	19.12	0.00	0.00	39.78	32.46	0.00	0.00	NB2 + SB6
A2	KSB	0.00	7.03	0.00	50.76	0.00	12.16	0.00	KB + SB6
A3	NKB	48.58	8.10	0.00	0.70	85.71	14.29	0.00	NB + KB
B1	NMB	0.51	0.00	51.72	0.00	0.98	0.00	99.02	MB6 + NB
B2		17.37	0.00	28.22	0.00	38.10	0.00	61.90	NB + NB2
C1	MSB	0.00	0.00	39.81	15.90	0.00	0.00	71.46	MB6 + SB6
D1	KMB	0.00	0.80	51.80	0.00	0.00	1.52	98.48	MB6 + KMB6
D2		0.00	4.88	44.33	0.00	0.00	9.92	90.08	KB + KMB6
E1	NKMB	0.51	0.78	51.27	0.00	0.97	1.48	97.55	NB + KMB6 + MB6
E2		5.47	3.49	43.00	0.00	10.53	6.72	82.76	NB + KMB6 + NB2
E3		21.85	6.39	25.53	0.00	40.64	11.88	47.48	KB + KMB6 + NB2
F1	NKSB	18.96	6.08	0.00	35.27	31.44	10.08	0.00	KB + NB2 + SB6
G1	NMSB	0.53	0.00	39.41	15.35	0.96	0.00	71.28	MB6 + NB + SB6
G2		16.96	0.00	6.70	33.95	29.44	0.00	11.63	SB6 + NB + NB2
H1	KMSB	0.00	0.57	36.30	15.19	0.00	1.09	69.73	MB6 + KMB6 + SB6
H2		0.00	4.68	16.71	34.41	0.00	8.39	29.95	KMB6 + KB + SB6
X	NKMSB	0.50	0.55	37.12	15.22	0.94	1.03	69.53	NB + KMB6 + MB6 + SB6
Y		17.15	5.45	5.12	30.18	29.62	9.41	8.84	SB6 + KB + KMB6 + NB2
Z		15.88	5.12	8.30	27.87	27.78	8.96	14.52	NB + NB2 + KMB6 + SB6

[a]Standard uncertainty is $u(T)$ = 0.1 K. Relative standard uncertainties for pressure and solubility are $u_r(p)$ = 0.05, $u_r[w(Na^+)]$ = 0.005, $u_r[w(K^+)]$ = 0.005, $u_r[w(Mg^{2+})]$ = 0.005, $u_r[w(Sr^{2+})]$ = 0.005, and $u_r[w(Br^-)]$ = 0.003. w(B): mass fraction of B. Abbreviations: NB = NaBr, NB2 = NaBr·2H_2O, MB6 = $MgBr_2$·6H_2O, SB6 = $SrBr_2$·6H_2O, KMB6 = KBr·$MgBr_2$·6H_2O, KB = KBr, NSB: NaBr−$SrBr_2$−H_2O, KSB: KBr−$SrBr_2$−H_2O, NKB: NaBr−KBr−H_2O, NMB: NaBr−$MgBr_2$−H_2O, MSB: $MgBr_2$−$SrBr_2$−H_2O, KMB: KBr−$MgBr_2$−H_2O, NKMB: NaBr−KBr−$MgBr_2$−H_2O, NKSB: NaBr−KBr−$SrBr_2$-H_2O, NMSB: NaBr−$MgBr_2$−$SrBr_2$−H_2O, KMSB: KBr−$MgBr_2$−$SrBr_2$−H_2O, NKMSB: NaBr−KBr−$MgBr_2$−$SrBr_2$−H_2O.

H_2O at 298 and 323 K, quaternary systems NaBr−$MgBr_2$−$SrBr_2$−H_2O and KBr−$MgBr_2$−$SrBr_2$−H_2O at 323 K and NaBr−KBr−$SrBr_2$−H_2O at 348 K were also carried out by our group.[19−21]

To date, phase equilibria in many systems containing potassium and bromide have been studied. The phase equilibrium studies of ternary system KCl−KBr−H_2O at 298, 313, and 333 K[22] aimed at the comprehensive development and utilization of potash resources in Vientiane Plain of Laos. Christov[23] made phase equilibrium experiments and theoretical studies of ternary system KBr−$MgBr_2$−H_2O at 323.15 K. Hu et al.[24] calculated the solubilities of salts in ternary system KBr−CsBr−H_2O at 298 K. Our group studied the phase equilibria in ternary system KBr−$K_2B_4O_7$−H_2O at 298, 323, 348, and 373 K;[25−28] ternary system NaBr−KBr−H_2O at 373 K;[29] quaternary system NaBr−KBr−$CaBr_2$−H_2O at 298 and 323 K;[30,31] quaternary system KBr−$SrBr_2$−$MgBr_2$−H_2O at 323 K;[20] quaternary system KCl−KBr−K_2SO_4−H_2O at 323, 348, and 373 K;[32−34] quaternary system KCl−KBr−$K_2B_4O_7$−H_2O at 323 K;[35] quaternary system KBr−$CaBr_2$−$MgBr_2$−H_2O at 298 and 323 K;[36] and quinary system KCl−KBr−K_2SO_4−$K_2B_4O_7$−H_2O at 323 and 348 K.[37] The studies of the above multitemperature phase equilibrium systems provided important data for the deep underground brine in the Sichuan basin.

Considering the characteristic of the deep underground brine in the western Sichuan basin, this work is designated to accurately determine solid−liquid equilibria of quinary system NaBr−KBr−$MgBr_2$−$SrBr_2$−H_2O at 323 K, which is a subsystem of the above-mentioned multicomponent brine system.

2. EXPERIMENTAL SECTION

2.1. Reagents and Instruments. The chemicals used in this work are listed in Table 1. The water used was deionized by the Ultrapure Water Instrument (UPT-II-20T, resistivity ≥ 17 MΩ cm). The thermostatic water bath oscillator (HZS-H, accurate to 0.1 K) and electronic balance (AL104, accurate to 0.0001 g) were used in the phase equilibrium experiments.

2.2. Experimental Methods. The isothermal dissolution equilibrium method was adopted in this work. All samples were prepared by referring to the invariant points of subsystems, and a new salt was added in appropriate proportion till supersaturation. For each univariant curve, 7−12 groups of samples were prepared, then put in a ground glass

DOI: 10.1021/acs.jced.9b00225
J. Chem. Eng. Data 2019, 64, 3436−3443

bottle, and placed in a thermostatic water bath oscillator with controlled temperature (323 ± 0.1 K). All samples were oscillated to reach the solid−liquid equilibrium state. The supernatant solution was regularly taken out for chemical analysis during oscillation in solid−liquid equilibrium, and the precipitation−dissolution equilibrium was identified by constant compositions of solution. The equilibrium time was about 20 days. The composition of the equilibrium liquid phase was analyzed by chemical analysis, and the equilibrium solid phase was determined by Schreinemakers wet-residue method.[38]

2.3. Analytical Methods. The analytical methods of each ion were as follows: Br^- was titrated by the silver nitrate volumetric method using potassium chromate as an indicator, with standard uncertainty 0.003 in mass fraction. K^+ was titrated by the sodium tetraphenylboron method using Titan Yellow as an indicator, with standard uncertainty 0.005 in mass fraction. When Mg^{2+} and Sr^{2+} coexisted, sodium hydroxide was added to precipitate Mg^{2+} as $Mg(OH)_2$ at first and then the free Sr^{2+} was titrated by the ethylenediaminetetraacetic acid (EDTA) volumetric method using KB as an indicator. When the complexation of Sr^{2+} with EDTA was completed, $Mg(OH)_2$ was dissolved using hydrochloric acid (1:1). The free Mg^{2+} was titrated by the EDTA volumetric method adding Eriochrome black T as an indicator. The standard uncertainties of Mg^{2+} and Sr^{2+} are 0.005 in mass fraction. Na^+ was evaluated by the ionic charge balance, with standard uncertainty 0.005 in mass fraction.

3. RESULTS AND DISCUSSION

3.1. The Quinary System NaBr−KBr−$MgBr_2$−$SrBr_2$−H_2O. The experimental data of invariant points of quinary system NaBr−KBr−$MgBr_2$−$SrBr_2$−H_2O and its quaternary and ternary subsystems at 323 K are listed in Table 2. Based on these data, taking J(NaBr) as the X-axis, J($MgBr_2$) as the Y-axis, and J(KBr) as the Z-axis, the dry-salt composition diagram of this system was drawn as a regular tetrahedron, as shown in Figure 1. The four vertices of the tetrahedron are aqueous solutions of four salt components NaBr, KBr, $MgBr_2$, and $SrBr_2$. The six edges represent six ternary subsystems, i.e., NaBr−KBr−H_2O, NaBr−$MgBr_2$−H_2O, NaBr−$SrBr_2$−H_2O, KBr−$MgBr_2$−H_2O, KBr−$SrBr_2$−H_2O, and $MgBr_2$−$SrBr_2$−H_2O. The four triangular side faces represent four quaternary subsystems, i.e., NaBr−KBr−$MgBr_2$−H_2O, NaBr−KBr−$SrBr_2$−H_2O, NaBr−$MgBr_2$−$SrBr_2$−H_2O, and KBr−$MgBr_2$−$SrBr_2$−H_2O. Points A1, A2, A3, and C1 are invariant points of ternary subsystems NaBr−$SrBr_2$−H_2O, KBr−$SrBr_2$−H_2O, NaBr−KBr−H_2O, and $MgBr_2$−$SrBr_2$−H_2O, respectively. Meanwhile, to show each crystallization region clearly, the three-dimensional (3D) stereogram of each crystallization region was drawn, as shown in Figure 2.

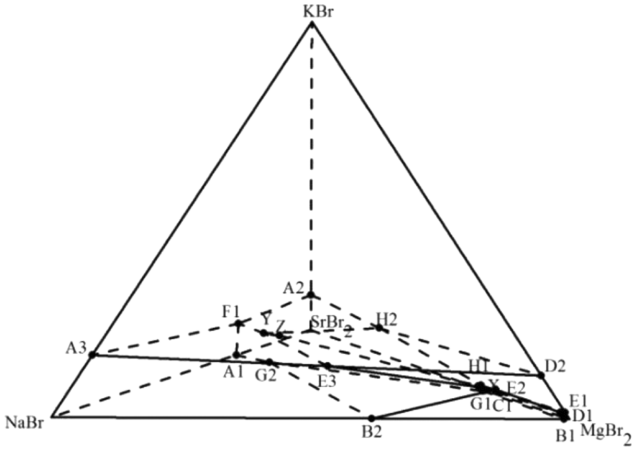

Figure 1. Three-dimensional stereogram of quinary system NaBr−KBr−$MgBr_2$−$SrBr_2$−H_2O at 323 K.

As can be seen in Figures 1 and 2 and Table 2, the quinary system has one complex salt KBr·$MgBr_2$·$6H_2O$ and three hydrated salts NaBr·$2H_2O$, $SrBr_2$·$6H_2O$, and $MgBr_2$·$6H_2O$ at 323 K. The isothermal equilibrium phase diagram consists of six crystallization regions (NaBr·$2H_2O$, NaBr, $SrBr_2$·$6H_2O$, $MgBr_2$·$6H_2O$, KBr, and KBr·$MgBr_2$·$6H_2O$), ten univariant curves (E1X, H1X, G1X, XZ, H2Y, F1Y, E3Y, YZ, G2Z, and E2Z), and three quinary invariant points (X, Y, and Z). The equilibrium liquid composition and solid phases of three quinary invariant points are as follows: (1) point X, saturated with $SrBr_2$·$6H_2O$, $MgBr_2$·$6H_2O$, KBr·$MgBr_2$·$6H_2O$, and NaBr; (2) point Y, saturated with $SrBr_2$·$6H_2O$, NaBr·$2H_2O$, KBr·$MgBr_2$·$6H_2O$, and KBr; (3) point Z, saturated with $SrBr_2$·$6H_2O$, NaBr, KBr·$MgBr_2$·$6H_2O$, and NaBr·$2H_2O$.

As can be seen in Figure 2, the crystallization region of KBr occupies the largest space, indicating that KBr has the lowest solubility, so it is the easiest to crystallize out of the saturated solution. The crystallization region of $MgBr_2$·$6H_2O$ occupies the smallest space, indicating that the solubility of $MgBr_2$·$6H_2O$ is the largest. Therefore, it is difficult for $MgBr_2$·$6H_2O$ to crystallize out of the saturated solution.

Many experimental results of phase equilibria show that among the systems involving $MgBr_2$, such as ternary system $MgBr_2$−$SrBr_2$−H_2O, quaternary systems NaBr−$MgBr_2$−$SrBr_2$−H_2O and KBr−$MgBr_2$−$SrBr_2$−H_2O,[24,25] and quinary system NaBr−KBr−$MgBr_2$−$SrBr_2$−H_2O, the solubility of $MgBr_2$ is the highest, so it has the strongest salting-out effect on other ions in solution. The salting-out effect can be attributed mainly to the high concentration and strong hydration of $MgBr_2$, which significantly reduces the activity of water in solution and thus decreases the solubilities of other salts. In addition, the high-concentration $MgBr_2$ also has a strong common-ion effect on the other salts.

3.2. The Saturation Surface of KBr in a Quinary System. The experimental data of quinary system NaBr−KBr−$MgBr_2$−$SrBr_2$−H_2O saturated with KBr at 323 K are summarized in Table 3. Taking J(NaBr) + J($MgBr_2$) + J($SrBr_2$) = 100 as a benchmark, the Jänecke indices were calculated as follows

$$J(\mathrm{B}) = 100\frac{w(\mathrm{B})}{w(\mathrm{NaBr}) + w(\mathrm{MgBr_2}) + w(\mathrm{SrBr_2})}$$

where B stands for one of the components of NaBr, $MgBr_2$, and $SrBr_2$. Based on the Jänecke indices in Table 3, the dry-salt composition diagram under the condition of KBr saturation can be obtained (Figure 3). It is the radial projection of the saturation surface of KBr. This projection was made from vertex KBr on the regular tetrahedron in Figure 1 to the base surface of the composition of NaBr−$MgBr_2$−$SrBr_2$.

As can be seen in Figure 3, the projection plane contains one invariant point (Y), three univariant curves (H2Y, F1Y, and E3Y), and three crystallization regions ($SrBr_2$·$6H_2O$, NaBr·$2H_2O$, and KBr·$MgBr_2$·$6H_2O$). Apparently, $SrBr_2$·$6H_2O$ has the largest crystallization region and KBr·$MgBr_2$·$6H_2O$ has the

DOI: 10.1021/acs.jced.9b00225
J. Chem. Eng. Data 2019, 64, 3436−3443

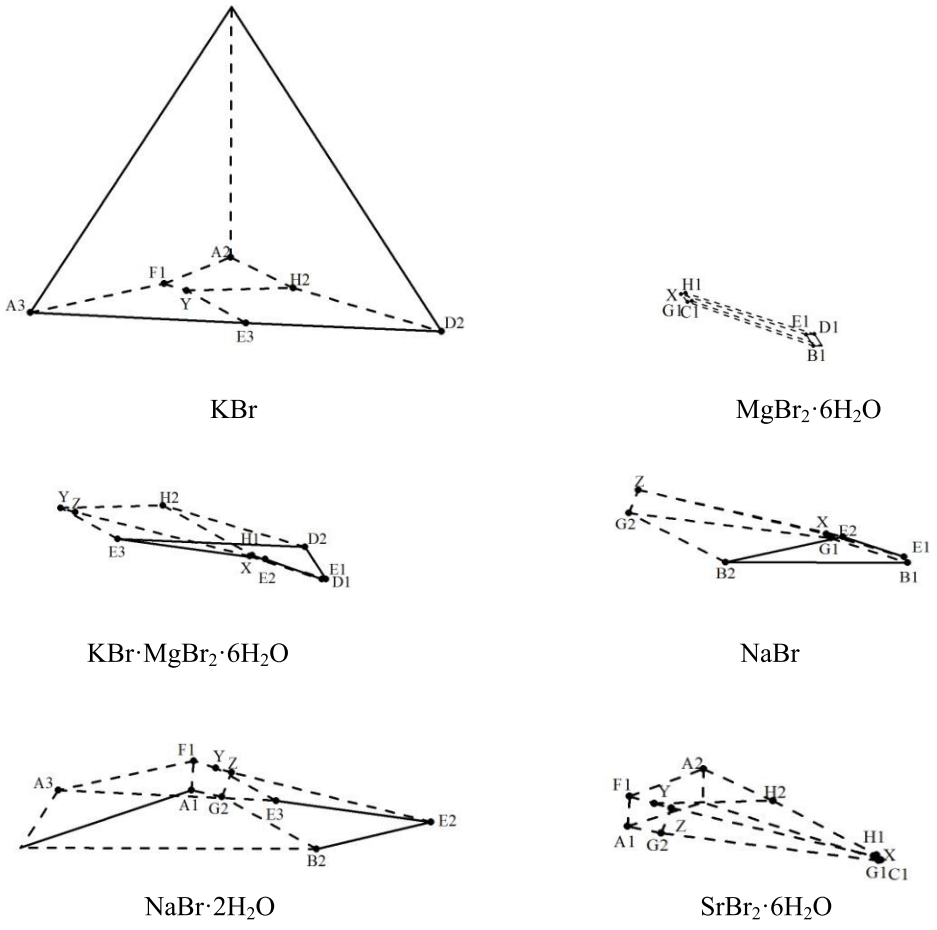

Figure 2. Three-dimensional stereograms of each crystallization region in quinary system NaBr−KBr−$MgBr_2$−$SrBr_2$−H_2O at 323 K.

Table 3. Compositions of Liquids in a Quinary System Saturated with KBr at 323 K and 0.09575 MPa[a]

	composition of solution w(B)[a] × 100				Jänecke index of dry salt J(NaBr) + J($MgBr_2$) + J($SrBr_2$) = 100				
no.	w(NaBr)	w(KBr)	w($MgBr_2$)	w($SrBr_2$)	J(NaBr)	J($MgBr_2$)	J(H_2O)	J(KBr)	equilibrium solids
1, H2	0.00	4.68	16.71	34.41	0.00	32.69	86.46	9.15	SB6 + KMB6 + KB
2	3.85	4.89	14.21	33.89	7.41	27.35	83.08	9.41	SB6 + KMB6 + KB
3	8.24	5.12	11.23	33.10	15.67	21.36	80.48	9.74	SB6 + KMB6 + KB
4	12.73	5.36	8.33	32.26	23.87	15.62	77.49	10.05	SB6 + KMB6 + KB
5, F1	18.96	6.08	0.00	35.27	34.96	0.00	73.19	11.21	NB2 + SB6 + KB
6	17.91	5.88	2.21	33.67	33.30	4.11	74.98	10.93	NB2 + SB6 + KB
7, E3	21.85	6.39	25.53	0.00	46.12	53.88	97.57	13.49	NB2 + KMB6 + KB
8	21.01	6.21	23.48	3.67	43.63	48.75	94.75	12.89	NB2 + KMB6 + KB
9	20.65	6.17	21.70	7.30	41.59	43.71	88.98	12.43	NB2 + KMB6 + KB
10	20.37	6.03	18.30	11.10	40.93	36.77	88.81	12.12	NB2 + KMB6 + KB
11	19.94	5.93	16.29	13.56	40.05	32.72	88.93	11.91	NB2 + KMB6 + KB
12	19.21	5.82	13.70	17.33	38.24	27.27	87.46	11.58	NB2 + KMB6 + KB
13	18.49	5.67	9.46	22.58	36.59	18.72	86.68	11.22	NB2 + KMB6 + KB
14	17.79	5.55	7.31	26.65	34.38	14.13	82.51	10.72	NB2 + KMB6 + KB
15, Y	17.15	5.45	5.12	30.18	32.70	9.76	80.27	10.39	NB2 + KMB6 + SB6 + KB

[a]Standard uncertainty is $u(T)$ = 0.1 K. Relative standard uncertainties for pressure and solubility are $u_r(p)$ = 0.05, $u_r[w(Na^+)]$ = 0.005, $u_r[w(K^+)]$ = 0.005, $u_r[w(Mg^{2+})]$ = 0.005, $u_r[w(Sr^{2+})]$ = 0.005, and $u_r[w(Br^-)]$ = 0.003. w(B): mass fraction of B. Abbreviations: NB2 = NaBr·$2H_2O$, SB6 = $SrBr_2$·$6H_2O$, KMB6 = KBr·$MgBr_2$·$6H_2O$, KB = KB.

smallest crystallization region, showing that under the condition of KBr saturation, the solubilities of other salts increase in the order of $SrBr_2$·$6H_2O$, NaBr·$2H_2O$, and KBr·$MgBr_2$·$6H_2O$.

3.3. The Saturation Surface of $SrBr_2$·$6H_2O$ in a Quinary System. The Jänecke dry-salt indices were calculated on the basis of J(NaBr) + J(KBr) + J($MgBr_2$) = 100, as shown in Table 4. Based on the data in Table 4, the

DOI: 10.1021/acs.jced.9b00225
J. Chem. Eng. Data 2019, 64, 3436−3443

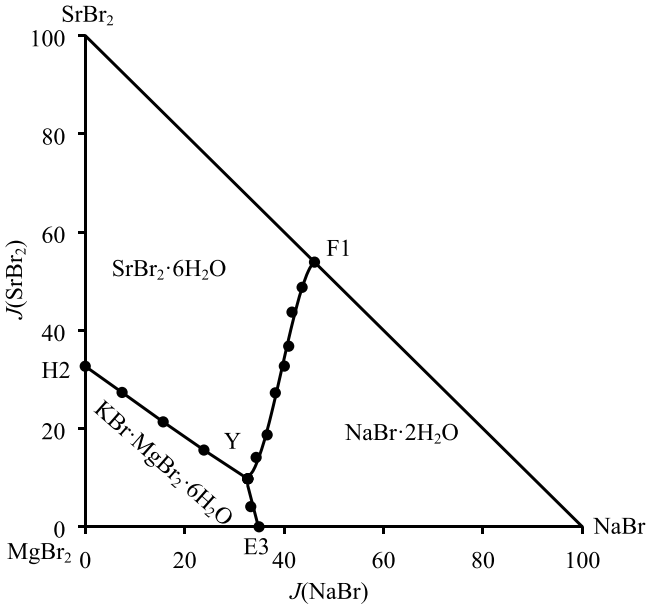

Figure 3. Projection of the saturation surface of KBr in a quinary system at 323 K.

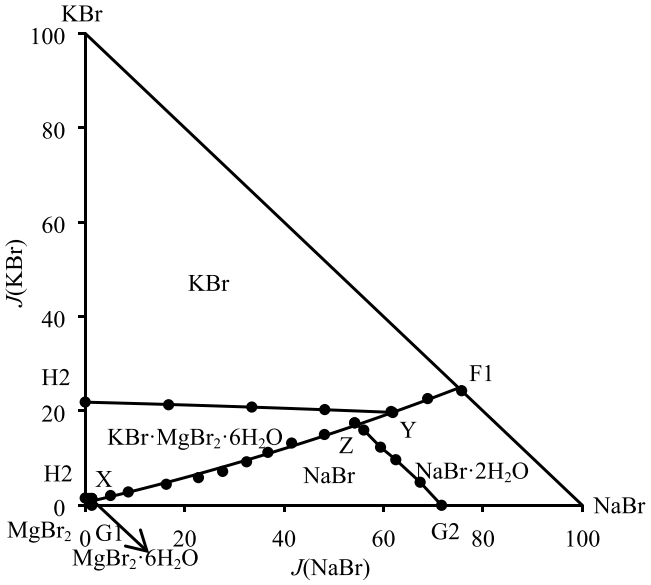

Figure 4. Projection of the saturation surface of $SrBr_2·6H_2O$ in a quinary system at 323 K.

corresponding dry-salt diagram under the condition of $SrBr_2·6H_2O$ saturation was drawn, as shown in Figure 4.

As can be seen in Figure 4, the projection plane of this quinary system under the condition of $SrBr_2·6H_2O$ saturation contains three invariant points (*X*, *Y*, and *Z*), seven univariant

Table 4. Compositions of Liquids in a Quinary System Saturated with $SrBr_2·6H_2O$ at 323 K and 0.09575 MPa[a]

	composition of solution $w(B)^a \times 100$				Jänecke index of dry salt $J(NaBr) + J(KBr) + J(MgBr_2) = 100$				
no.	$w(NaBr)$	$w(KBr)$	$w(MgBr_2)$	$w(SrBr_2)$	$J(NaBr)$	$J(KBr)$	$J(H_2O)$	$J(SrBr_2)$	equilibrium solids
1, F1	18.96	6.08	0.00	35.27	75.72	24.28	158.51	140.85	KB + NB2 + SB6
2	17.91	5.88	2.21	33.67	68.88	22.62	155.12	129.50	KB + NB2 + SB6
3, Y	17.15	5.45	5.12	30.18	61.87	19.66	151.88	108.87	KMB6 + KB + NB2 + SB6
4, Z	15.88	5.12	8.30	27.87	54.20	17.47	146.18	95.12	NB + NB2 + KMB6 + SB6
5	14.72	4.59	11.28	25.82	48.12	15.00	142.50	84.41	NB + KMB6 + SB6
6	13.25	4.21	14.45	24.31	41.52	13.19	137.20	76.18	NB + KMB6 + SB6
7	12.02	3.67	17.02	23.52	36.75	11.22	133.81	71.90	NB + KMB6 + SB6
8	10.88	3.09	19.55	22.18	32.46	9.22	132.16	66.17	NB + KMB6 + SB6
9	9.43	2.45	22.23	21.44	27.65	7.18	130.31	62.86	NB + KMB6 + SB6
10	7.92	2.04	24.81	20.23	22.78	5.87	129.42	58.18	NB + KMB6 + SB6
11	5.78	1.58	28.09	19.45	16.30	4.46	127.22	54.87	NB + KMB6 + SB6
12	3.15	1.03	32.18	18.11	8.66	2.83	125.22	49.81	NB + KMB6 + SB6
13	1.89	0.77	34.44	16.67	5.09	2.08	124.61	44.93	NB + KMB6 + SB6
14, X	0.50	0.55	37.12	15.22	1.31	1.44	122.11	39.87	NB + KMB6 + MB6 + SB6
15	0.32	0.55	36.92	15.20	0.85	1.46	124.40	40.22	MB6 + KMB6 + SB6
16, H1	0.00	0.57	36.30	15.19	0.00	1.55	130.02	41.20	MB6 + KMB6 + SB6
17, G1	0.53	0.00	39.41	15.35	1.33	0.00	111.94	38.43	MB6 + NB + SB6
18	0.51	0.38	38.77	15.30	1.29	0.96	113.57	38.58	MB6 + NB + SB6
19, G2	16.96	0.00	6.70	33.95	71.68	0.00	179.16	143.49	NB + NB2 + SB6
20	16.81	1.22	6.92	32.22	67.37	4.89	171.66	129.14	NB + NB2 + SB6
21	16.68	2.58	7.44	30.78	62.47	9.66	159.25	115.28	NB + NB2 + SB6
22	16.49	3.42	7.85	28.27	59.40	12.32	158.39	101.84	NB + NB2 + SB6
23	16.02	4.56	8.01	27.05	56.03	15.95	155.16	94.61	NB + NB2 + SB6
24, H2	0.00	4.68	16.71	34.41	0.00	21.88	206.64	160.87	KMB6 + KB + SB6
25	3.85	4.89	14.21	33.89	16.78	21.31	191.76	147.67	KMB6 + KB + SB6
26	8.24	5.12	11.23	33.1	33.51	20.82	176.74	134.61	KMB6 + KB + SB6
27	12.73	5.36	8.33	32.26	48.18	20.29	162.64	122.10	KMB6 + KB + SB6

[a]Standard uncertainty is $u(T) = 0.1$ K. Relative standard uncertainties for pressure and solubility are $u_r(p) = 0.05$, $u_r[w(Na^+)] = 0.005$, $u_r[w(K^+)] = 0.005$, $u_r[w(Mg^{2+})] = 0.005$, $u_r[w(Sr^{2+})] = 0.005$, and $u_r[w(Br^-)] = 0.003$. $w(B)$: mass fraction of B. Abbreviations: NB = NaBr, NB2 = $NaBr·2H_2O$, MB6 = $MgBr_2·6H_2O$, SB6 = $SrBr_2·6H_2O$, KMB6 = $KBr·MgBr_2·6H_2O$, KB = KBr.

DOI: 10.1021/acs.jced.9b00225
J. Chem. Eng. Data 2019, 64, 3436−3443

Table 5. Compositions of Liquids in a Quinary System Saturated with $MgBr_2·6H_2O$ at 323 K and 0.09575 MPa[a]

	composition of solution w(B)[a] × 100				Jänecke index of dry salt J(NaBr) + J(KBr) + J($SrBr_2$) = 100				
no.	w(NaBr)	w(KBr)	w($MgBr_2$)	w($SrBr_2$)	J(NaBr)	J(KBr)	J(H_2O)	J($MgBr_2$)	equilibrium solids
1, G1	0.53	0.00	39.41	15.35	3.34	0.00	281.55	248.17	SB6 + NB + MB6
2	0.51	0.38	38.77	15.30	3.15	2.35	278.20	239.47	SB6 + NB + MB6
3, X	0.50	0.55	37.12	15.22	3.07	3.38	286.48	228.15	SB6 + KMB6 + NB + MB6
4	0.32	0.55	36.92	15.20	1.99	3.42	292.53	229.74	SB6 + KMB6 + MB6
5, H1	0.00	0.57	36.30	15.19	0.00	3.62	304.19	230.33	SB6 + KMB6 + MB6
6, E1	0.51	0.78	51.27	0.00	39.53	60.47	3677.52	3974.42	NB + KMB6 + MB6
7	0.50	0.76	50.20	0.18	34.72	52.78	3358.33	3486.11	NB + KMB6 + MB6
8	0.50	0.73	49.13	0.39	30.86	45.06	3040.12	3032.72	NB + KMB6 + MB6
9	0.50	0.70	47.87	0.73	25.91	36.27	2601.04	2480.31	NB + KMB6 + MB6
10	0.50	0.68	46.45	1.21	20.92	28.45	2140.59	1943.51	NB + KMB6 + MB6
11	0.50	0.65	44.32	1.78	17.06	22.18	1800.34	1512.63	NB + KMB6 + MB6
12	0.50	0.63	42.16	2.97	12.20	15.37	1310.73	1028.29	NB + KMB6 + MB6
13	0.50	0.60	40.08	4.21	9.42	11.30	1028.44	754.80	NB + KMB6 + MB6
14	0.50	0.58	38.77	7.38	5.91	6.86	623.76	458.27	NB + KMB6 + MB6

[a]Standard uncertainty is $u(T)$ = 0.1 K. Relative standard uncertainties for pressure and solubility are $u_r(p)$ = 0.05, $u_r[w(Na^+)]$ = 0.005, $u_r[w(K^+)]$ = 0.005, $u_r[w(Mg^{2+})]$ = 0.005, $u_r[w(Sr^{2+})]$ = 0.005, and $u_r[w(Br^-)]$ = 0.003. w(B): mass fraction of B. Abbreviations: NB = NaBr, MB6 = $MgBr_2·6H_2O$, SB6 = $SrBr_2·6H_2O$, KMB6 = $KBr·MgBr_2·6H_2O$.

curves (G1X, H1X, H2Y, XZ, YZ, F1Y, and G2Z), and five crystallization regions ($MgBr_2·6H_2O$, $KBr·MgBr_2·6H_2O$, $NaBr·2H_2O$, NaBr, and KBr). KBr has the largest crystallization region, whereas $MgBr_2·6H_2O$ is with the smallest crystallization region, indicating that under the condition of $SrBr_2·6H_2O$ saturation, KBr has the minimum solubility and is easier to crystallize out of the saturated solution; $MgBr_2·6H_2O$ has the maximum solubility with no easier occurrence of crystallization and precipitation.

3.4. The Saturation Surface of $MgBr_2·6H_2O$ in a Quinary System. Using J(NaBr) + J(KBr) + J($SrBr_2$) = 100 as a benchmark, the Jänecke indices were obtained (Table 5). Meanwhile, the dry-salt diagram under the condition of $MgBr_2·6H_2O$ saturation was drawn, as shown in Figure 5.

As can be seen in Figure 5, the projection plane consists of one invariant point (X), three univariant curves (H1X, G1X, and XE1), and three crystallization regions ($SrBr_2·6H_2O$, NaBr, and $KBr·MgBr_2·6H_2O$). NaBr has the largest crystallization region, whereas $SrBr_2·6H_2O$ has the smallest crystallization region. The above results show that NaBr has the minimum solubility and is easier to crystallize out of the saturated solution. As opposed to NaBr, $SrBr_2·6H_2O$ has the maximum solubility and is more difficult to crystallize.

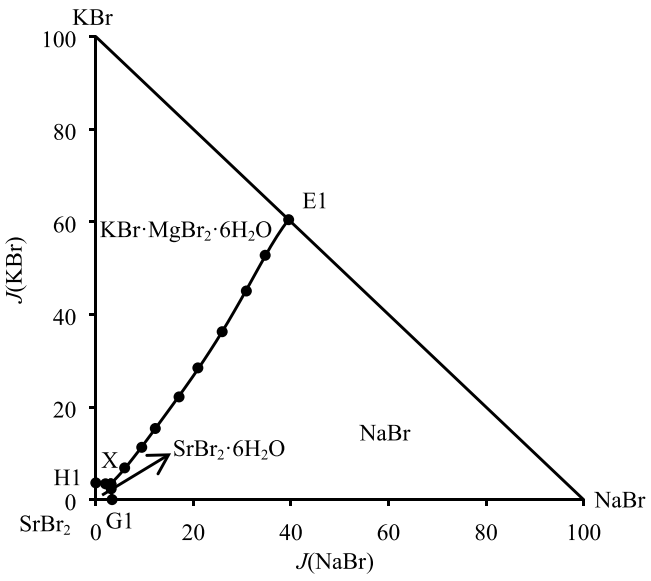

Figure 5. Projection of the saturation surface of $MgBr_2·6H_2O$ in a quinary system at 323 K.

3.5. The Saturation Surface of $NaBr·2H_2O$ in a Quinary System. Using J(KBr)+J($MgBr_2$)+J($SrBr_2$) = 100 as a benchmark, the Jänecke indices of all salts and H_2O can be obtained (Table 6). Meanwhile, the projection of dry-salt compositions under the condition of $MgBr_2·6H_2O$ saturation was shown in Figure 6.

As can be seen in Figure 6, the projection plane consists of two invariant points (Y and Z), five univariant curves (E3Y, F1Y, YZ, E2Z, and G2Z), and four crystallization regions ($SrBr_2·6H_2O$, NaBr, $NaBr·2H_2O$, and $KBr·MgBr_2·6H_2O$). The crystallization regions of KBr and $KBr·MgBr_2·6H_2O$ are the largest and the smallest, respectively. That is, KBr has the minimum solubility, so it is easy to crystallize from the saturated solution; $KBr·MgBr_2·6H_2O$ has the maximum solubility and thus it is not easy to crystallize.

4. CONCLUSIONS

To promote comprehensive development and utilization of bromine-containing brine resources, guide the design process of separation and purification of inorganic salts, and provide a theoretical basis for understanding the geochemical processes involving relevant brine-mineral systems, the stable phase equilibria of quinary system NaBr−KBr−$MgBr_2$−$SrBr_2$−H_2O were investigated at 323 K by the method of isothermal dissolution. Meanwhile, the three-dimensional composition diagram and its two-dimensional projection diagrams under the conditions of KBr, $SrBr_2·6H_2O$, $MgBr_2·6H_2O$, and $NaBr·2H_2O$ saturation were drawn and analyzed. As an important supplement to the study of the underground brine system in the Sichuan basin, the research results of this paper will produce great economic and social effects on the basis of guiding industrial production.

DOI: 10.1021/acs.jced.9b00225
J. Chem. Eng. Data 2019, 64, 3436−3443

Table 6. Compositions of Liquids in a Quinary System Saturated with $NaBr·2H_2O$ at 323 K and 0.09575 MPa[a]

	composition of solution $w(B)$[a] × 100				Jänecke index of dry salt $J(KBr) + J(MgBr_2) + J(SrBr_2) = 100$				
no.	$w(NaBr)$	$w(KBr)$	$w(MgBr_2)$	$w(SrBr_2)$	$J(KBr)$	$J(MgBr_2)$	$J(H_2O)$	$J(SrBr_2)$	equilibrium solids
1, F1	18.96	6.08	0.00	35.27	14.70	0.00	95.99	85.30	KB + NB2 + SB6
2	17.91	5.88	2.21	33.67	14.08	5.29	96.58	80.63	KB + NB2 + SB6
3, Y	17.15	5.45	5.12	30.18	13.37	12.56	103.31	74.06	SB6 + KB + KMB6 + NB2
4, E3	21.85	6.39	25.53	0.00	20.02	79.98	144.83	0.00	NB2 + KMB6 + KB
5	21.01	6.21	23.48	3.67	18.62	70.38	136.78	11.00	NB2 + KMB6 + KB
6	20.65	6.17	21.70	7.30	17.54	61.70	125.62	20.76	NB2 + KMB6 + KB
7	20.37	6.03	18.30	11.10	17.02	51.65	124.75	31.33	NB2 + KMB6 + KB
8	19.94	5.93	16.29	13.56	16.57	45.53	123.76	37.90	NB2 + KMB6 + KB
9	19.21	5.82	13.70	17.33	15.79	37.18	119.24	47.03	NB2 + KMB6 + KB
10	18.49	5.67	9.46	22.58	15.04	25.09	116.15	59.88	NB2 + KMB6 + KB
11	17.79	5.55	7.31	26.65	14.05	18.50	108.07	67.45	NB2 + KMB6 + KB
12, Z	15.88	5.12	8.30	27.87	12.40	20.10	103.73	67.50	NB + NB2 + KMB6 + SB6
13	14.72	4.89	11.38	25.72	11.65	27.10	103.10	61.25	NB + KMB6 + NB2
14	13.25	4.61	17.45	21.31	10.63	40.24	100.02	49.14	NB + KMB6 + NB2
15	12.32	4.37	21.02	18.52	9.95	47.87	99.68	42.18	NB + KMB6 + NB2
16	10.88	4.16	24.65	15.48	9.39	55.66	101.22	34.95	NB + KMB6 + NB2
17	9.43	3.85	30.68	10.44	8.56	68.22	101.40	23.22	NB + KMB6 + NB2
18	7.72	3.68	38.41	3.43	8.08	84.38	102.72	7.54	NB + KMB6 + NB2
19, E2	5.47	3.49	43.00	0.00	7.51	92.49	103.33	0.00	NB + KMB6 + NB2
20, G2	16.96	0.00	6.70	33.95	0.00	16.48	104.28	83.52	SB6 + NB+ NB2
21	16.81	1.22	6.92	32.22	3.02	17.15	106.12	79.83	SB6 + NB+ NB2
22	16.68	2.58	7.44	30.78	6.32	18.24	104.22	75.44	SB6 + NB+ NB2
23	16.49	3.42	7.85	28.27	8.65	19.85	111.20	71.50	SB6 + NB+ NB2
24	16.02	4.56	8.01	27.05	11.51	20.22	111.96	68.27	SB6 + NB+ NB2

[a]Standard uncertainty is $u(T) = 0.1$ K. Relative standard uncertainties for pressure and solubility are $u_r(p) = 0.05$, $u_r[w(Na^+)] = 0.005$, $u_r[w(K^+)] = 0.005$, $u_r[w(Mg^{2+})] = 0.005$, $u_r[w(Sr^{2+})] = 0.005$, and $u_r[w(Br^-)] = 0.003$. $w(B)$: mass fraction of B. Abbreviations: NB = NaBr, NB2 = $NaBr·2H_2O$, SB6 = $SrBr_2·6H_2O$, KMB6 = $KBr·MgBr_2·6H_2O$.

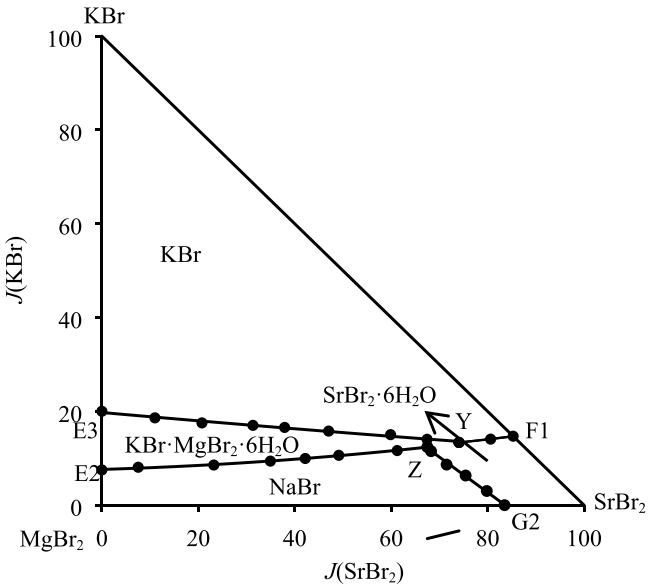

Figure 6. Projection of the saturation surface of $NaBr·2H_2O$ in a quinary system at 323 K.

AUTHOR INFORMATION

Corresponding Author

*E-mail: sangshihua@sina.com.cn, sangsh@cdut.edu.cn. Tel: +086-13032845233.

ORCID

Shi-Hua Sang: 0000-0002-5948-3882

Rui-Zhi Cui: 0000-0001-6861-8227

Notes

The authors declare no competing financial interest.

ACKNOWLEDGMENTS

This project was supported by the National Natural Science Foundation of China (41873071) and Scientific Research and Innovation Team in Universities of Sichuan Provincial Department of Education (15TD0009). We would also like to thank the editors and reviewers for their valuable comments and suggestions.

REFERENCES

(1) Lin, Y. T. Resource Advantages of the Underground Brines of Sichuan Basin and the Outlook of Their Comprehensive Exploitation (in Chinese). *J. Salt Lake Res.* **2006**, *14*, 1−8.

(2) Wang, S. L.; Zheng, M. P. Discovery of Triassic Polyhalite in Changshou Area of East Sichuan Basin and Its Genetic Study (in Chinese). *Miner. Deposits* **2014**, *33*, 1045−1056.

(3) Han, S. H.; Shui, P.; Yu, C.; Qiu, Z. G. Present Situation and Sustainable Development Suggestion of Chinese Strontium Resource Industry (in Chinese). *Bull. Sci. Technol.* **2018**, *34*, 1−5.

(4) Zheng, M. P.; Zhang, Z.; Hou, X. H.; Lin, Y. J. The Prospects and the Mining Development Strategy of Potassium Resources in China (in Chinese). *Land Res. Inf.* **2015**, *10*, 3−9.

(5) Chen, X. N.; Wang, H. Z. Bromine Resource and Analysis of the Industry Development (in Chinese). *J. Salt Chem. Ind.* **2013**, *42*, 4−7.

(6) Lin, Y. T.; Chen, S. L. Exploration and Development Prospect of Underground Brine in Sichuan Basin (in Chinese). *J. Salt Lake Res.* **2008**, *16*, 1−7.

DOI: 10.1021/acs.jced.9b00225
J. Chem. Eng. Data 2019, 64, 3436−3443

(7) Balarew, C.; Christov, C.; Valyashko, V.; Petrenko, S. Thermodynamics of Formation of Carnallite Type Double Salts. *J. Solution Chem.* **1993**, *22*, 173−181.
(8) Christov, C. Study of Bromide Salts Solubility in the $(m_1KBr + m_2CaBr_2)_{(aq)}$ System at T = 323.15 K. Thermodynmic Model of Solution Behaviour and (Solid + Liquid) Equilibria in the Ternaries $(m_1KBr + m_2CaBr_2)_{(aq)}$, and $(m_1MgBr_2 + m_2CaBr_2)_{(aq)}$, and in the Quinary (Na + K + Mg + Ca + Br + H_2O) Systems to High Concentration and Temperature. *J. Chem. Thermodyn.* **2012**, *55*, 7−22.
(9) Assarsson, G. O. Equilibria in Aqueous Systems Containing Na^+, K^+, Sr^{2+} and Cl^-. *J. Phys. Chem. A* **1953**, *57*, 207−210.
(10) Assarsson, G. O.; Balder, A. Equilibria in Aqueous Systems Containing Na^+, K^+, Sr^{2+}, Ca^{2+} and Cl^- Between 18 °C and 114 °C. *J. Phys. Chem. A* **1954**, *58*, 253−255.
(11) Assarsson, G. O.; Balder, A. Equilibria Between 18 °C and 100 °C in the Aqueous Systems Containing Sr^{2+}, Mg^{2+} and Cl^-. *J. Phys. Chem. A* **1954**, *58*, No. 416.
(12) Assarsson, G. O.; Balder, A. The Poly-Component Aqueous Systems Containing the Chlorides of Ca^{2+}, Mg^{2+}, Sr^{2+}, K^+ and Na^+ Between 18 °C and 93 °C. *J. Phys. Chem. A* **1955**, *59*, 631−633.
(13) Blidin, V. P. Heterogeneous Equilibrium in Aqueous Ternary Systems of Lithium Chloride and the Chlorides of Barium, Strontium and Calcium (in Russ.). *Dokl. Akad. Nauk SSSR* **1952**, *84*, 947−950.
(14) Filippov, V. K.; Fedorov, Y. A.; Charykov, N. A. Thermodynamics of Phase Equilibria in the Potassium, Strontium, Sodium, Chloride, Water (K^+, Sr^{2+}/Cl^--H_2O, Na^+, Sr^{2+}/Cl^--H_2O and Na^+, K^+, Sr^{2+} /Cl^--H_2O) System at 25 °C (in Russ.). *Zh. Obshch. Khim.* **1990**, *60*, 492−499.
(15) Ding, X. P.; Sun, B.; Shi, L. J.; Yang, H. T.; Song, P. S. Study on Phase Equilibria in NaCl-$SrCl_2$-H_2O Ternary System at 25 °C (in Chinese). *Inorg. Chem. Ind.* **2010**, *42*, 9−11.
(16) Shi, L. J.; Sun, B.; Ding, X. P.; Song, P. S. Phase Equilibria in Ternary System KCl-$SrCl_2$-H_2O at 25 °C (in Chinese). *Chin. J. Inorg. Chem.* **2010**, *26*, 333−338.
(17) Bi, Y. J.; Sun, B.; Zhao, J.; Song, P. S.; Li, W. Phase Equilibrium in Ternary System $SrCl_2$-$CaCl_2$-H_2O at 25 °C (in Chinese). *Chin. J. Inorg. Chem.* **2011**, *27*, 1765−1771.
(18) Zhang, X.; Sang, S. H.; Zhong, S. Y.; Zhao, X. P. Equilibria in the Ternary System $SrCl_2$-KCl-H_2O and the Quaternary System $SrCl_2$-KCl-NaCl-H_2O at 323 K. *Russ. J. Phys. Chem. A.* **2015**, *89*, 2322−2326.
(19) Liu, Q.; Gao, Y. Y.; Zhang, W. Y.; Sang, S. H. Solid-Liquid Equilibria in the Ternary Systems $SrBr_2$-$MgBr_2$-H_2O at (298 and 323) K. *J. Chem. Eng. Jpn.* **2018**, *51*, 1−5.
(20) Liu, Q.; Gao, Y. Y.; Sang, S. H.; Cui, R. Z.; Zhang, X. P. Solid-Liquid Equilibria in the Quaternary Systems NaBr-$SrBr_2$-$MgBr_2$-H_2O and KBr-$SrBr_2$-$MgBr_2$-H_2O at 323 K. *J. Chem. Eng. Data* **2017**, *62*, 1264−1268.
(21) Hu, J. X.; Sang, S. H.; Zhang, T. T.; Wang, D. Solid-Liquid Equilibria in the Systems $CaBr_2$-$MgBr_2$-H_2O and NaBr-KBr-$SrBr_2$-H_2O at 348 K. *J. Chem. Eng. Data* **2015**, *60*, 3087−3092.
(22) Weng, Y. B.; Wang, Y. F.; Wang, J. K.; Yin, Q. X. Phase Diagram for the Ternary System of K^+/Cl^-, Br^--H_2O at 298 K, 313 K and 333 K (in Chinese). *J. Chem. Eng. Chin. Univ.* **2007**, *21*, 695−699.
(23) Christov, C. Isopiestic Investigation of the Osmotic Coefficients of $MgBr_{2(aq)}$ and Study of Bromide Salts Solubility in the $(m_1KBr + m_2MgBr_2)_{(aq)}$ System at T = 323.15 K. Thermodynamic Model of Solution Behaviour and (Solid + Liquid) Equilibria in the $MgBr_{2(aq)}$, and $(m_1KBr + m_2MgBr_2)_{(aq)}$ Systems to High Concentration and Temperature. *J. Chem. Thermodyn.* **2011**, *43*, 344−353.
(24) Hu, B.; Song, P. S.; Li, H. X.; Li, W. Solubility Prediction in the Ternary Systems NaCl-RbCl-H_2O, KCl-CsCl-H_2O and KBr-CsBr-H_2O at 25 °C Using the Ion-Interaction Model. *CALPHAD* **2007**, *31*, 541−544.
(25) Sang, S. H.; Yin, H. A.; Ni, S. J.; Zhang, C. J. A Study on Equilibrium Solubilities and Properties of Solutions in the Ternary System $K_2B_4O_7$-KBr-H_2O at 298 K (in Chinese). *J. Chengdu Univ. Technol.* **2006**, *33*, 414−416.
(26) Zhao, X. Y.; Sang, S. H.; Sun, M. L. Phase Equilibrium of the Ternary System $K_2B_4O_7$-KBr-H_2O at 323 K (in Chinese). *J. Salt Lake Res.* **2011**, *19*, 35−39.
(27) Sang, S. H.; Li, T.; Cui, R. Z. A Study on Phase Equilibria in the Ternary Salt-Water System KBr-$K_2B_4O_7$-H_2O at 348 K (in Chinese). *J. Salt Lake Res.* **2013**, *21*, 29−32.
(28) Cui, R. Z.; Sang, S. H.; Hu, Y. X.; Hu, J. W. Phase Equilibria in the Ternary Systems KBr-$K_2B_4O_7$-H_2O and KCl-$K_2B_4O_7$-H_2O at 373 K. *Acta Geol. Sin.* **2014**, *87*, 1668−1673.
(29) Sang, S. H.; Cui, R. Z.; Hu, Y. X. Phase Equilibria of Two Ternary Systems NaBr-Na_2SO_4-H_2O and NaBr-KBr-H_2O at 373 K (in Chinese). *J. Chem. Eng. Chin. Univ.* **2014**, *28*, 939−943.
(30) Cui, R. Z.; Sang, S. H.; Li, D. W.; Liu, Q. Z. Measurements and Calculations of Solid-Liquid Equilibria in the Quaternary System NaBr-KBr-$CaBr_2$-H_2O at 298 K. *CALPHAD* **2015**, *49*, 120−126.
(31) Cui, R. Z.; Wang, W.; Yang, L.; Sang, S. H. Phase Diagram of Quaternary System NaBr-KBr-$CaBr_2$-H_2O at 323 K. *Russ. J. Phys. Chem. A.* **2018**, *92*, 475−481.
(32) Wang, D.; Sang, S. H.; Zeng, X. X.; Ning, H. Y. Phase Equilibrium of KCl-KBr-K_2SO_4-H_2O Quaternary System at 323 K (in Chinese). *Petrochem. Technol.* **2011**, *40*, 285−288.
(33) Zhang, K. J.; Sang, S. H.; Li, T.; Cui, R. Z. Liquid-Solid Equilibria in the Quaternary System KCl-KBr-K_2SO_4-H_2O at 348 K. *J. Chem. Eng. Data* **2013**, *58*, 115−117.
(34) Cui, R. Z.; Sang, S. H.; Hu, Y. X. Solid-Liquid Equilibria in the Quaternary Systems KCl-KBr-$K_2B_4O_7$-H_2O and KCl-KBr-K_2SO_4-H_2O at 373 K. *J. Chem. Eng. Data* **2013**, *58*, 477−481.
(35) Hu, Y. X.; Sang, S. H.; Cui, R. Z.; Wang, Y. Solid-Liquid Equilibria in the Quaternary System KCl-KBr-$K_2B_4O_7$-H_2O at 323 K. *J. Chem. Eng. Data* **2014**, *59*, 1886−1891.
(36) Cui, R. Z.; Wang, Z. C.; Xu, J. S.; Sang, S. H. Measurements and Calculations of Solid-Liquid Equilibria in the Quaternary System KBr-$CaBr_2$-$MgBr_2$-H_2O at (298 and 323) K. *Fluid Phase Equilib.* **2017**, *450*, 140−148.
(37) Cui, R. Z.; Sang, S. H.; Li, T.; Zhang, Y. G. Phase Equilibria in the Quinary System KCl-KBr-K_2SO_4-$K_2B_4O_7$-H_2O at 323 K and 348 K (in Chinese). *J. Chem. Ind. Eng.* **2013**, *64*, 827−833.
(38) Fosbøl, P. L.; Thomsen, K.; Stenby, E. H. Reverse Schreinemakers Method for Experimental Analysis of Mixed-Solvent Electrolyte Systems. *J. Solution Chem.* **2009**, *38*, 1−14.

DOI: 10.1021/acs.jced.9b00225
J. Chem. Eng. Data 2019, 64, 3436−3443